Cells and Materials

Volume 7 | Number 1 Article 2

1997

A Quantitative Method of Measuring Cell-Substrate Adhesion Areas

R. G. Richards
AO/ASIF Research Institute

G. Rh Owen
AO/ASIF Research Institute

B. A. Rahn
AO/ASIF Research Institute

I. ap Gwynn
The University of Wales

Cells and Materials Vol. 7, No. 1, 1997 (pages 15-30) 1051-6794/97$5.00+.25
Scanning Microscopy International, Chicago (AMF O'Hare), IL 60666 USA

A QUANTITATIVE METHOD OF MEASURING CELL-SUBSTRATE ADHESION AREAS

R.G. Richards[1*], G.Rh. Owen[1], B.A. Rahn[1] and I. ap Gwynn[2]

[1]AO/ASIF Research Institute, Clavadelerstrasse, CH 7270 Davos, Switzerland
[2]Institute of Biological Sciences, The University of Wales, Aberystwyth, SY23 3DA, Wales, U.K.

(Received for publication June 6, 1997 and in revised form September 9, 1997)

Abstract

Variability in measurements of the 'cell adhesion strength' of fibroblasts to substrates using mechanical disruption techniques causes difficulty in determining precisely the position, in the cytoskeleton-focal adhesion-matrix-substrate interface, where failure has occurred. In the present study, a quantitative *in vitro* procedure for measuring the total area and percentage of fibroblast adhesion to biomaterials, using the scanning electron microscope (SEM), is described. The amount of adhesion of L929 and Balb/c3T3 fibroblasts to discs of stainless steel, commercially pure titanium, and polyethylene terepthalate (Thermanox) was quantified. Cells were fixed, stained with heavy metals, dehydrated and embedded in resin. The resin blocks were removed from the substrate and sputter coated. The samples were examined in a field emission SEM using backscattered electron imaging. Demonstration that the cells had been removed with their adhesion sites, was by immunocytochemical labelling of vinculin within the focal adhesions of the embedded cells. Quantification of cell adhesion was performed by measuring the total area of each cell (imaged at 15 kV) and the area of their adhesion sites (imaged at 4kV) using an image analysis system. The *in vitro* results show (under static conditions, with the materials, roughnesses and cell types used) that roughness does not affect the total area of adhesion. The procedure could be applied to any cells that form focal adhesions, such as osteoblasts and may be developed to assess connective tissue adhesion to implant surfaces from *in vivo* experiments.

Key Words: Field emission scanning electron microscopy, backscattered electron imaging, immuno-labelling, cell adhesion, image analysis.

*Address for correspondence:
R.G. Richards
AO/ASIF Research Institute,
Clavadelerstrasse, CH 7270 Davos Platz, Switzerland
Telephone Number: 0041 81 414 2397
FAX Number: 0041 81 414 2288
E-mail: geoff.richards@ao-asif.ch

Introduction

Most cells require to be anchored for growth and survival. Anchorage is accomplished by adhering to neighbouring cells and or to an extracellular matrix (ECM) of macromolecules, first observed as a micro-exudate secreted upon contact with surfaces (Rosenberg, 1960). Different mechanisms are in operation for cell-cell and cell-ECM adhesion, respectively. The ECM helps to hold the cells and tissues together, providing an organised lattice for cell migration and interaction. In connective tissues the ECM is abundant and takes most of the stress that the tissue is subjected to. The cells are attached to components of the matrix, on which they may exert a force.

The cell-matrix adhesions mechanically connect the internal actin filaments to the matrix. The complex is known as a focal adhesion, focal plaque or focal contact. Contacts between cells and solids were first observed using the surface contact light microscope (Ambrose, 1956) and their distance of closest approach to the surface was found to be approximately 10 nm using interference reflection microscopy (Curtis, 1964). It was not until the late sixties that a transmission electron microscope (TEM) was used to observe cell contacts (Cornell, 1969), confirming their distance of closest approach. Cultured fibroblasts hold onto the ECM on the substratum at the focal adhesions exerting a traction onto it with their cytoskeleton (Isenberg *et al.*, 1976). The same mechanism is thought to occur naturally *in vivo* onto implanted biomaterials. Focal adhesions are frequently considered to be artefacts of tissue culturing *in vitro* since they are less prominent *in vivo*. *In vitro* focal adhesions have a planar con-figuration imposed by the rigid substrate, which is similar to the imposition made by an implant *in vivo*. Fibroblasts grown in collagen gels lack discernible focal adhesions, which is in agreement with this interpretation. The ECM can influence the organisation of a cell's cytoskeleton and the intercellular actin fibres can influence the orientation of secreted matrix. The ECM may therefore cause cell orientation, as may variations in the topography of the implant surfaces. An understanding of fibroblast cell adhesion, and a quantifiable method of measuring it will

be of use in biocompatibility studies of soft tissues to biomaterial implant surfaces.

Measurements of fibroblast adhesion

Mechanical methods. The first published method of measuring cell adhesion was by Coman (1944). The force required to separate epithelial cells is estimated by the bending of a micropipette, attached to one cell by suction, which reaches a maximum just before separation. The method is unsuited to a study of more than a few individual cells.

Leonard Weiss (1961) hypothesised: "if the cohesive strength of the cell surface is less than the adhesive strength of the cell/substratum joint then on distraction, rupture will occur in the cell surface, part of which will be left on the cell substratum". From this he suggested that during cell movement, if cell ruptures continually occur, then pieces of the cell surface will remain adherent to the substratum. He suggested that it is unlikely that the force required to distract one cell from another is the same as the force of adhesion between the two cells. He studied the detachment of fibroblasts from a flat surface by producing a tangential hydrodynamic force with a rotating disc above them. The force produced is maximum at the edge of the disc and minimal in the centre and can be increased by increasing the viscosity of the fluid, the rotation speed of the disc or by decreasing the distance between the discs. The adhesion could be measured over a range of forces from the centre to the periphery. The final estimate of adhesive strength may vary with the rate of the application of the distractive force as well as its magnitude. It was shown that secondary cultures of cells are less easily detached from the sites where cells had previously been detached. He suggested that physical variations in the method of adhesion measurement can produce marked variation in the final estimate. Weiss and Coombs (1963) later showed that a proteinaceous antigenic material ruptures off cells when the cells are distracted from glass by mechanical force. They were unsure if the material remained after cell distraction or if it was a microexudate. Bell (1978) demonstrated that the force required to separate a cell from a surface, is of the same order of magnitude as the force required to pull integral membrane proteins out of the cell membrane.

Vaishnav *et al.* (1983) determined local erosion stress of endothelium using a jet impingement method. Jets of physiological saline are impinged at right angles to an endothelium causing annular lesions to be formed, observed by staining. The endothelium can withstand large normal stresses from impingement, but is eroded by the shear stresses from the jet. The erosion stress is calculated from the external radius of the lesion and the shear stress expected at that distance from the impinging jet. Bundy *et al.* (1994) produced a quantitative *in vitro* method of measuring differences in fibroblast adhesion strength to biomaterials using a modified version of the jet impingement method (Vaishnav *et al.*, 1983). A strong shear stress is produced from a fluid forced through a thin needle. This created a lesion in the cell layer, where it is of sufficient magnitude to detach cells. By measuring the size of the lesion and using stress versus radial distance calculations (Vaishnav *et al.*, 1983) the stresses required to erode off the intact cell layer can be determined. The only statistical difference in the results is found between all materials (titanium, steel, graphite, polystyrene and a cobalt based alloy Haynes 25) and glass. It was necessary to question whether the failure in the cell layer is an intrinsic cohesive failure within the fibroblasts or separation at the cell/ECM or ECM/substrate interface. The authors questioned whether the results correlated with earlier *in vivo* peel testing (Bundy *et al.*, 1991). In the earlier *in vivo* study they subjected stainless steel and plasma sprayed pure titanium implants that had been implanted into mice to tissue peel tests, using a customised device. The results showed that plasma sprayed titanium is much more adherent to the tissue than electropolished stainless steel. This difference is presumed to be due to roughness differences. Scanning electron microscopy (SEM) revealed that the interface failure sometimes occurred in the cell multilayers. No difference between the two metals in respect to cell adherence is observed using the jet impingement testing. This could be interpreted as meaning that the jet impingement measurement reveals the degree of cell adherence up until the cell/ECM interfacial strength exceeds the cell's own cohesive strength. To question whether the failure in the cell layer is an intrinsic cohesive failure within the fibroblasts or separation at the cell/ECM or ECM/substrate interface during microjet impingement, an SEM analysis of the cellular remainders was performed. Test surfaces of steel, titanium and plastic Thermanox were used (Richards *et al.*, 1995a). Cellular remainders, consisting of membranes, the adhesion sites and some cytoskeleton are observed where the shear forces of the impingement had ruptured the cells. This shows, with the highly adherent surfaces looked at, that cell cohesion in fibroblasts is weaker than the adhesion strength to the substrate. This reiterated the difficulty in determining the position of molecular failure in cell-substrate adhesion measurements when mechanical techniques are used to remove cells.

Truskey and Pirone (1990) looked at the effect of fluid shear stress on cell adhesion and observed that non spread cells attach weakly and are easily removed following the onset of flow. During long term flow, fluid shear stresses alter the shape, orientation and

mechanical properties of the cell and the distribution of its focal adhesions. Exposure to flow reduces the attachment strength. The actual force on the cell during exposure to the flow could not be determined because the precise shape of the cell is not known, though estimates could be made. Truskey and Proulx (1993) characterised cellular interactions with cell detachment induced by laminar shear stress. They examined whether smaller, rounder cells are easier to detach by laminar flow, and whether detachment occurs by dissociation of adhesion proteins and their membrane receptors or by rupture of the membrane. Cell detachment by membrane rupture is found to be a significant mechanism of cell detachment at higher shear stresses.

Van Kooten *et al.* (1991) developed a chamber attached to an image analysis system to observe cells exposed to flow *in vitro*, also allowing their area, perimeter, and shape as a function of duration and strength of shear stress to be determined. They later showed that fibroblast cells with greater areas of spread stayed longer on the substrate in the laminar flow (Van Kooten *et al.*, 1992). During exposure to flow cells rounded up before detaching. They also looked at exposure to fluid shear in a flow chamber, using endothelial cells on glass(Van Kooten *et al.*, 1994). They found that both 3 and 24 hour adhesion times gave rise to comparable cell retention levels after 2 hours of flow. They concluded that after 3 hours adhesion, adhesion strength does not significantly increase with time during the following 21 hours.

Hertl *et al.* (1984) used a centrifugal method of cell adhesion measurement to show that adhesiveness of single cell layers is about 30% more than that of multilayers, implying that cell-cell attachments are weaker than cell-substrate attachments. Bongrand and Goldstein (1983) showed that there is no distinction as to whether the strength of specific or non-specific bonds is being measured during cell detachment. The strength of initial cell adhesion using centrifugal force based measurements shows the adhesions are ten times stronger after the initial 15 minutes of adhesion time (Lotz *et al.*, 1989).

Real time measurements of cell-substratum adhesion, by focal adhesions can be obtained using tandem scanning confocal microscopy (Davies *et al.*, 1993). Focal adhesions are sharply defined in living cells at low radiance levels of the illuminating laser, so that images can be enhanced, digitised and isolated from other cellular detail. Focal adhesion area and the closeness of contact are measured with an image analysis system and used to define the adhesion of a cell or field of cells and show changes of cell adhesion, in real time. Subtraction of consecutive images showed continuous remodelling of individual focal adhesions occur in periods of less than 1 minute, though total cell adhesion varies by less than 10% over extended time periods. The focal adhesion regions are observed to be dynamic structures.

When reviewing the abundant literature on the attempts to measure the actual 'cell adhesion strength' of fibroblasts to substrates, it soon becomes apparent that variability in the measurements obtained makes it very difficult to obtain a reliable quantitative assessment of the 'adhesion strength'. The major variability may well arise not only as a result of the difficulty in determining precisely the position, in the cytoskeleton-focal adhesion-ECM-substrate interface, where failure has occurred during mechanical disruption, but also from the type of method used to make the measurements. From the SEM analysis of cell remainders after mechanical disruption of cells, using the microjet impingement method (Richards *et al.*, 1995a), it would appear that the weakest link in the chain lies within the cytoskeleton or within the cytoskeleton-focal adhesion interface. Therefore, during the mechanical disruption the actual strength of cell adhesion is not being measured. Until a study is performed which can show exactly where within the cell-surface interface rupture occurs, that it occurs in all focal adhesions within a cell at the same position and that it is found at the same position within all the cells in a population, then measurements of fibroblast cell adhesion strength, based on the use of mechanical disruption methods, can have little meaning.

Non-mechanical methods. Internal reflection microscopy, adapted for studying cell adhesion by Curtis (1964), showed differences in the area of cell adhesion sites to the substrate correlated closely with results of cell substratum adhesion strength observed (Lotz *et al.*, 1989). Both results show an adhesive strengthening during the initial cell attachment. This is thought to be produced by adhesion molecules coupling to the actin cytoskeleton at the adhesion site during the strengthening period. Hunter *et al.* (1995) studied the cell attachment and growth of fibroblasts and osteoblasts on prospective (polyethersulphone (PES), polyetherketone) and currently used orthopaedic biomaterials (titanium 318 alloy, cobalt chrome molybdenum alloy, ultra high molecular weight polyethylene (UHMWPE)). Attachment is assessed by indirect immunofluorescent labelling of vinculin, quantifying the degree of cell attachment by determining the mean number of focal adhesions containing vinculin, and using an image analysis system to determine the mean total area of the focal adhesions per cell. Attachment of fibroblasts to UHMWPE is significantly less than to the other materials. Tissue culture plastic generates a significantly higher numbers of focal adhesions and a larger area of vinculin localisation per cell than any of the other materials tested, except for the

titanium 318 alloy. There is no significant difference in the adhesion of osteoblasts to the different materials. SEM shows that fibroblast cells, with the greatest number and area of focal adhesions, are well spread and flattened. Those with the least number and area of focal adhesions are more rounded and less spread. SEM also shows few observable differences between the osteoblast cells on any of the materials.

The only two non-mechanical methods of quantifying cell adhesion (Lotz *et al.*, 1989; Hunter *et al.*, 1995), are based on light microscopy (LM) techniques and therefore have the limitations of resolution associated with their detecting system.

In the study presented here a quantitative method of measuring the total area and percentage of cell adhesion using SEM is described. In this method mechanical rupture was used only to remove cells which had been embedded in resin for support, leaving their adhesion sites still intact but removed from the substrates. That the method used allowed the removal of intact cells with their adhesion sites complete was demonstrated by the subsequent positive immunocytochemical labelling of the focal adhesion proteins. Differential contrast staining of the adhesion sites, by osmium and ruthenium reagents, made it possible to count and measure the areas of the adhesion, by means of computer-aided image analysis. It is hypothesised, as in the work of Lotz *et al.* (1989) and Hunter *et al.* (1995), that the compatibility of a biomaterial to soft tissues is deemed to be better when the area of actual cell adhesion is greater.

Materials and Methods

Cell culturing technique

L929 and Balb /c 3T3 fibroblastic cells were maintained according to the method of Elvin and Evans (1982). Stock cultures were recovered from a liquid nitrogen refrigerator and were plated at 300,000 cells per 25 cm^2 plastic flask in Dulbecco's Modified Eagle's Medium (DMEM) with 10% foetal calf serum, without antibiotics. After 3 days cells were detached with 0.25% trypsin and 0.02% EDTA (ethylenediaminetetraacetic acid) in TBSS (Tyrode buffered saline solution) - calcium and magnesium free. Detached cells were recovered, rinsed and cultured on 13 mm discs at an inoculum of 30,000 cells per well for 24 hours, not to confluency. Discs were commercially pure titanium (ISO 5832/2; Mathys Medical, Bettlach, Switzerland) or steel (ISO 5832/1; Mathys Medical) as used in orthopaedic implants or polyethylene terepthalate (Thermanox, (Th); Life Technologies, Basel, Switzerland). Three roughnesses were used: Steel 80 grit (S8), Titanium 80 grit (Ti8), Steel 600 grit (S6), Titanium 600 grit (Ti6), Steel 1000 grit (S1) and Titanium 1000 grit (Ti1) fabricated with abrasive paper becoming more smooth respectively. All metal discs were ultrasonically cleaned in deionized water and ethanol and then sterilised in a steam autoclave at 135°C for 10 minutes. The Thermanox discs were purchased pre-sterilised. The 80 grit metals had an average roughness height (peak to valley) (Rtm) of 15 μm, 600 grit had an Rtm of 3μm and 1000 grit had an Rtm of 2μm, as measured with an optical profilometer.

Preparation for electron microscopy

Fixation was carried out at 20°C. The cell culture medium was removed and the cells were rinsed for 2 minutes in 0.1 mol l^{-1} PIPES (piperazine-NN'-bis-2-ethane sulphonic acid) buffer pH 7.4. The cells were primarily fixed in 2.5% glutaraldehyde with 4% paraformaldehyde in 0.1 mol l^{-1} PIPES pH 7.4 for 5 minutes. The cells were rinsed three times for 2 minutes each in 0.1 mol l^{-1} PIPES pH 7.4 before postfixation in 0.5% osmium tetroxide with filtered ruthenium red (1500 ppm) in 0.1 mol l^{-1} PIPES pH 6.8 for 60 minutes. The cells were then rinsed three times for 2 minutes each in double distilled water and stained with 5% aqueous uranyl acetate for 60 minutes.

Each fixed cell culture was taken through an ethanol series - 50%, 60%, 70%, 80%, 90%, and 100% for 5 minutes respectively, followed by LR (London Resin) White (London Resin Co., Basingstoke, Hampshire, UK) resin for 1 hour for infiltration into the cells. The discs were removed and placed in 15 mm wells in a silicone mould to allow easy and clean removal of the resin blocks after polymerisation. Fresh resin was poured onto them with a drop of paraffin oil on the surface to exclude oxygen from the resin and was cured thermally at 65°C for 12-16 hours.

The resin blocks, containing the cells, were removed from the mould and excess resin was cleaned from the disc with a sharp knife and an abrasive paper. Thermanox discs were removed with a sharp knife, whilst metal discs were removed by rapid cooling on an aluminum block that had been kept in nitrogen slush at -210°C under vacuum (Richards *et al.*, 1995b). The specimens were then mounted onto stubs and coated at a low sputtering rate of 0.1 nm/s with 6 nm of gold/palladium 80/20 (as measured with a quartz thin film monitor) in a Baltec (Balzers, Liechtenstein) MED 020 unit.

Microscope operating conditions

SEM examination of the specimens was performed with a Hitachi (Tokyo, Japan) S-4100 field emission SEM fitted with a Autrata yttrium aluminum garnet (YAG) backscattered electron (BSE) detector (Prophysics, Uster, Switzerland) and a Quartz PCI image acquisition system (Quartz Imaging, Vancouver, Canada). The microscope was operated in BSE detection

mode at high emission currents (Richards and ap Gwynn, 1995) to display the highly stained focal adhesion sites directly on the undersurface of the cells within the embedding resin. The microscope was operated at an accelerating voltage of 15 kV and 4 kV at 50 μA emission current. A working distance of 10 mm was used to optimise both resolution and BSE collection. The condenser lens current was maximised (C18), thus minimising the spot size and the widest objective aperture of 100μm diameter (number 1) was used to allow more electrons to interact with the specimen. All images were stored in their original digital form.

Image and statistical analysis

Digital images were analysed with an image analysis and measurement system (PC-Image, Foster Findlay, Newcastle, UK). The system was calibrated to the dimensions of a scale bar on each image processed, to convert pixels to square microns (μm^2). The high kV image of a whole cell was thresholded to create a binary image, which was placed as an overlay upon the original image. The binary overlay was edited manually to define the region of interest around the periphery of the cell and data was recorded. The lower kV image, of the same cell, which displayed areas of adhesion sites, was thresholded to highlight the adhesion sites and a binary image of the region of interest placed in an overlay upon it. The area of the whole cell from the high kV image and of adhesion sites from the low kV image were measured. This whole procedure was repeated three times for each cell to check for errors, which could occur during manual editing of the binary image. The mean of the measurements from the three separate runs was calculated and the results subjected to statistical analysis. The results were first analysed using the Kolmogorov-Smirnov test for normality and a test of homogeneity of variances before performing an ANOVA (analysis of variance) test. If a difference between all the samples was found to be significant, then individual groups were analysed with the Tukey *post hoc* test (or honestly significant difference test). All tests were performed using the SPSS (Statistical Package for the Social Sciences, SPSS, Chicago, IL) computer statistics package.

Immunocytochemistry

Some fibroblasts cultured on Thermanox discs underwent immunolabelling. Optimisation of the method (after Hodges *et al.*, 1984 and Holgate *et al.*, 1983 for the silver enhancement) specifically to immunolabel the vinculin sites within the fibroblasts, for viewing with the field emission SEM (FESEM), led to the finalised method below.

All procedures were carried out at 20°C. The buffer used was 0.1 mol l^{-1} PIPES at pH 7.4. The cells were first rinsed for 1 minute in buffer, fixed in 4% paraformaldehyde in buffer, for 5 minutes and then rinsed six times for 30 seconds in buffer, + 1% bovine serum albumin (BSA). Cells were then permeabilised in 0.1% Triton X-100, diluted in double distilled water, for 3 minutes and then rinsed for 1 minute in buffer. Non-specific binding sites were blocked with 5% rabbit serum in buffer, + 1% BSA for 5 minutes. The cells were then incubated with 50μl of mouse anti-human vinculin (Sigma, St. Louis, MO, USA) at dilutions of 1:200 and 1:300 in buffer + 1% BSA + 0.1% Tween 20 for 1 hour. Cells were rinsed six times for 30 seconds each in buffer + 1% BSA + 0.1% Tween 20. The cells were then labelled with 50 μl of rabbit anti-mouse 1 nm gold conjugate (Biocell, Cardiff, UK) at 1:200 dilution in buffer + 1% BSA + 0.1% Tween 20 for 2 hours. All samples were then rinsed six times, each for 30 seconds in buffer and fixed in 2.5% glutaraldehyde for 5 minutes in buffer, before being rinsed again six times for 30 seconds in buffer. The immunolabelled cells were covered with 0.75 mol l^{-1} Tris acetate, three times for 1 minute each, which was then removed from the sample. Active silver reagent was prepared at a ratio of 1:1 solution A:B. Solution A (50ml) - Silver lactate 100 mg in 1 mol l^{-1} Citric acid at pH 7.4. Solution B (50 ml) - Hydroquinone 900 mg in 1 mol l^{-1} Citric acid at pH 7.4. Samples were covered with active silver reagent for 10 minutes, the reaction being terminated by a rinse in distilled water. The cells were postfixed with 0.02% OsO_4 in buffer (pH 6.8) for 1 hour and dehydrated through an ethanol series and critically point dried, as before. Samples were coated as before, some with 6 nm aluminum, which has a low density. Some samples that had been viewed from their upper surface were embedded in LR White resin. The discs were removed and the resin coated with 6 nm aluminum. The embedded cells were imaged with the SEM in BSE detection mode at high emission current (Richards and ap Gwynn, 1995).

Some fibroblasts cultured on Thermanox discs were used for immunocytochemical labelling of their focal adhesion sites for LM imaging. The method used was the same as for immunocytochemical labelling for SEM apart from: The secondary antibody incubation was either with (a) rabbit anti-mouse 5 nm gold conjugate or with (b) rabbit CY3 (orange, same excitation wavelength as rhodamine; DAKO, Copenhagen, Denmark) anti-mouse antibody for 2 hours. Samples incubated with rabbit CY3 anti-mouse antibody were not silver enhanced. Samples were mounted under glass coverslips using glycerol. Examination was with a Zeiss (Oberkochen, Germany) fluorescence microscope in

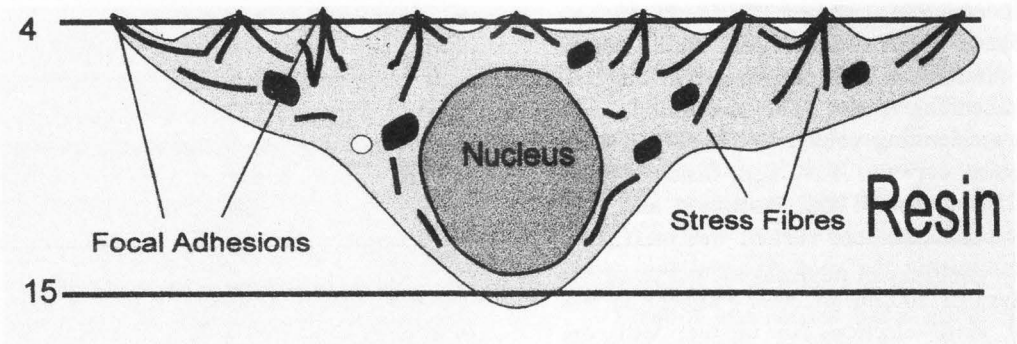

Figure 1. Diagrammatic representation of the general distribution of heavy metal stained contact areas and stress fibres in a cross section of the cell-substrate interface, after the substrate has been removed from the embedding resin. The two lines across the cell represent approximate regions of maximum depth from where BSE would be expected to emerge from at 4 and 15 kV respectively. Only a short depth into the contact interface can be observed at 4 kV, while details of the whole cell shape and size can be observed at 15 kV.

fluorescence mode, for cells labelled with CY3 conjugated antibody and in normal light mode for cells labelled with gold conjugated antibody. Some of the samples incubated with rabbit CY3 anti-mouse antibody were examined and photographed with a Molecular Dynamics (Sunnyville, CA) SARASTRO 2000 confocal microscope (Courtesy of Professor Charles Archer, University of Wales, Cardiff).

Results

BSE images of the cell undersurfaces were obtained using the high emission current operating mode of the FESEM, which increases the number of primary electrons available to interact with the specimen. This induces a greater production of BSE, which allows imaging at both the high and low accelerating voltage of the primary beam. By selecting a suitable accelerating voltage it was possible to control the maximum depth in a specimen from which the BSE emerged. The higher beam energy of 15 kV enabled visualisation of the whole cell size and shape, the BSE having emerged from the whole depth of the cell. The lower beam energy of 4 kV provided an image exclusively of the regions of the cell in contact with the substrate, i.e., the focal adhesions. In this case the BSE emerged from a very short distance within the highly stained focal adhesion sites at the cell surface (Fig. 1). There was very little primary beam penetration and there was no trace of the underlying cells.

The high density heavy metal stains gave a general contrast to the cells as a whole, the cells being surrounded by low density resin, which enhanced the definition of the cell peripheries (Fig. 2a). The stains were concentrated on the structural elements within the cells, which were surrounded by lesser-stained cellular matrix. Therefore at low beam energy, with low sample penetration, the highly stained focal adhesions had high contrast compared to the surrounding lower density cellular material and resin (Fig. 2b). The BSE images bore close resemblance to images of the distribution of adhesion sites within cells indirectly immunolabelled against vinculin (Figs. 3 and 4). Adhesion patterns of both cell types were viewed, either with LM for indirect immuno-fluorescent labelling, or with both LM and SEM for silver enhanced immunogold labelling. The patterns of adhesion were different for different cells within both cell type groups. Adhesion sites were less densely distributed in well spread out cells compared to smaller, rounded cells. CY3 immunolabelling of vinculin showed the general distribution of focal adhesions at the cell periphery and under the nucleus (Fig. 3a). This was also observed at the cell-substrate interface with an optical section taken with a confocal microscope (Fig. 3b). Immunogold labelling of vinculin followed by silver enhancement for viewing with the LM, again showed a similar pattern of focal adhesion sites to the immunofluorescent labelling (Fig. 3c).

Aluminum coating, which has a low density, was used to maintain high image contrast between the silver enhanced gold labels and the fibroblasts in the SEM. It was much more difficult to coat with aluminum than the more usual gold/palladium, since small fluctuations in vacuum pressure (optimally 6 x 10^{-3} bar for the Baltec MED 020 unit) or coating current (optimally 130 mA) would cause the target to etch the specimen. Before coating, the unit had to be operated without specimens in order to remove the oxides from the targets. The high emission current BSE imaging provided high contrast visualisation of the silver enhanced gold particles within

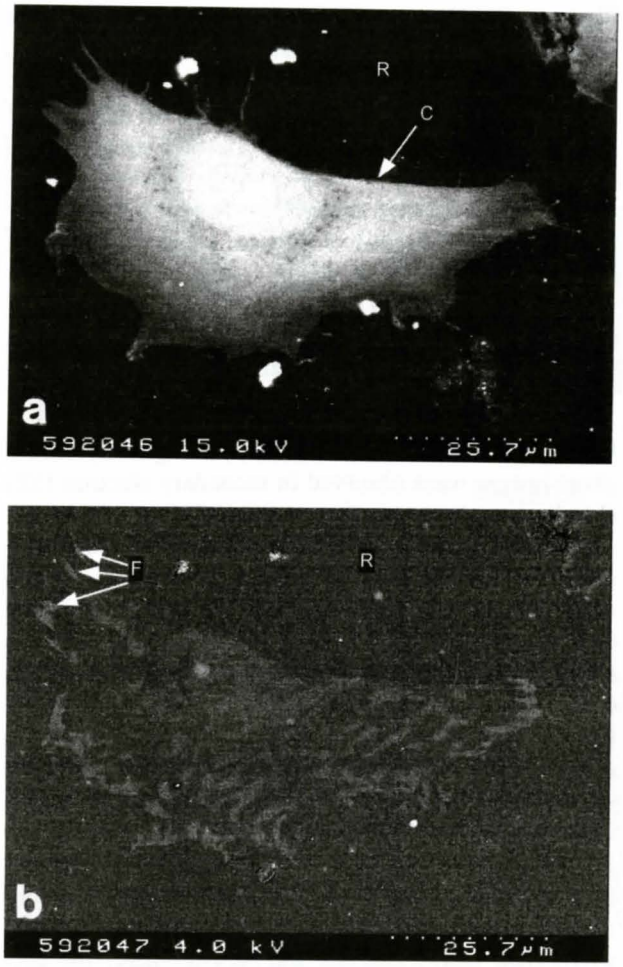

Figure 2. High contrast BSE image of the undersurface of a Balb c/3T3 fibroblast that had been cultured on Thermanox plastic and embedded within resin (R). (**a**) The high accelerating voltage of 15 kV caused deep beam penetration into the sample, and enabled visualisation of the cell (C) shape and size, (**b**) The low accelerating voltage of 4 kV caused little beam penetration into the sample so that only areas of highly stained cellular material close to the surface were observed, the focal adhesion sites (F).

---

the stained cellular material (Fig. 4). The gold label had increased from the original 1 nm size to between 50-150 nm during the silver enhancement period. When gold particles were close together they sometimes fused during silver enhancement to give the appearance of one large particle. A control with no primary antibody, under the same conditions as the labelling but with buffer used instead of label, showed very little gold was sticking to the cell and negligible amounts to the substrate (not shown).

After parameter optimisation of the labelling, such

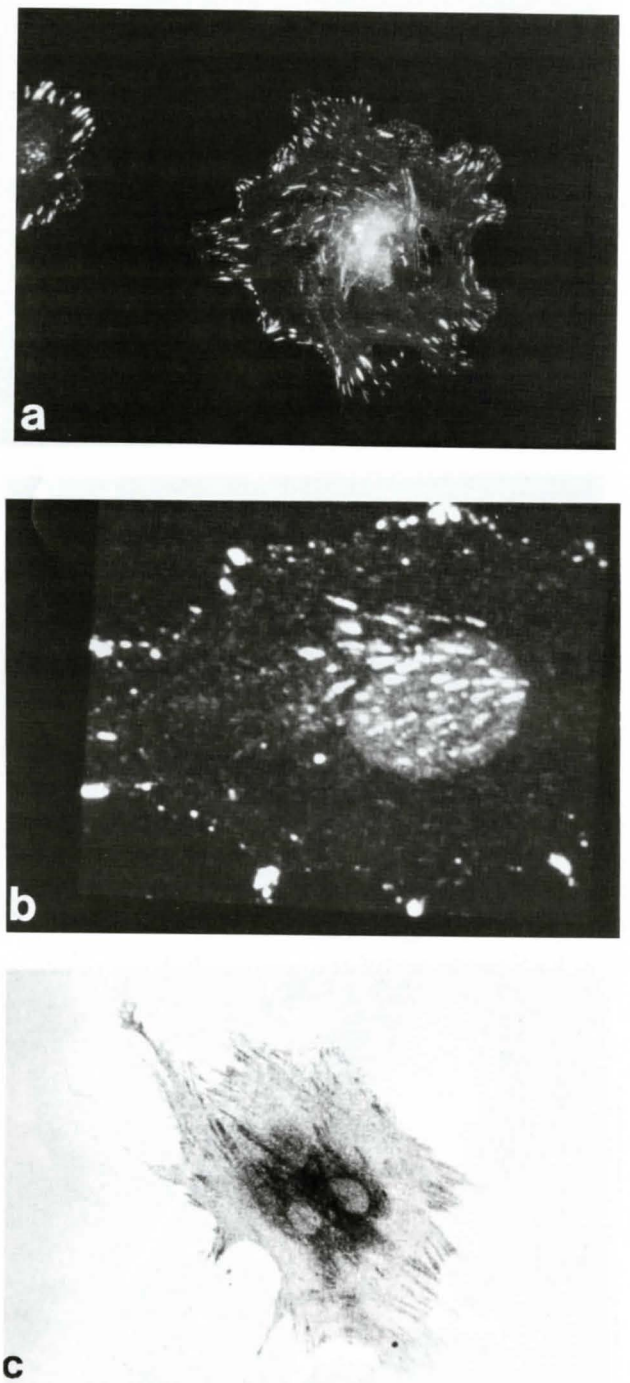

Figure 3. Light microscope images of immunolabelled focal adhesion sites. All three images, produced by different methods showed adhesion sites (arrows) around the cell peripheries and in the centre of the cells. (**a**) an L929 fibroblast with CY3 fluorescent labelled vinculin. (**b**) an optical section of a Balb c/3T3 fibroblast with CY3 fluorescent labelled vinculin taken with a confocal microscope. (**c**) An L929 fibroblast indirectly immunogold labelled against vinculin, silver enhanced for light microscope visualisation. Bar = 0.5 mm.

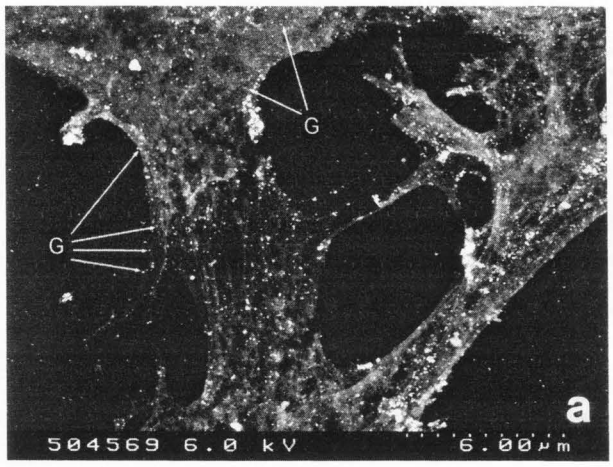

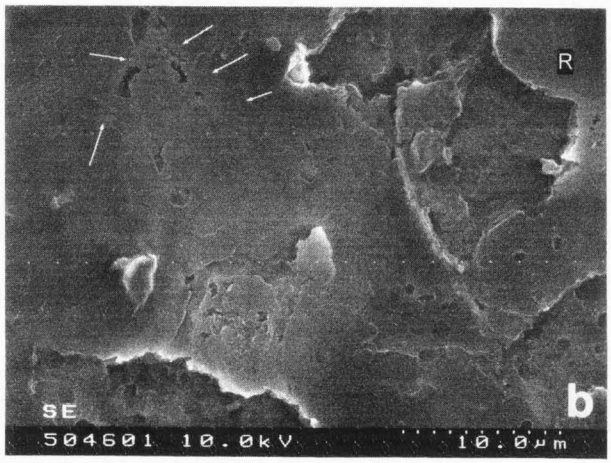

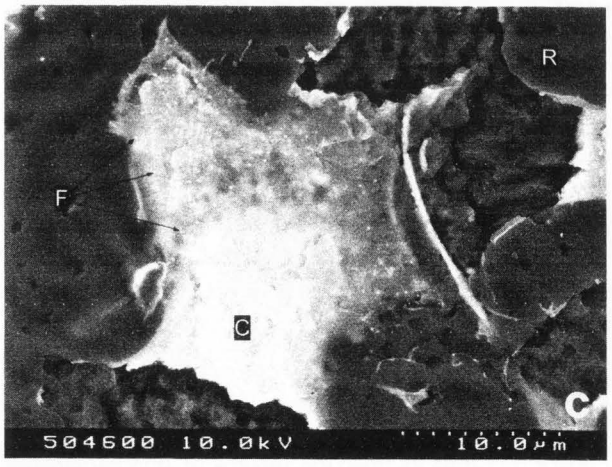

Figure 4. FESEM images produced with high emission current detection of focal adhesion sites immunogold labelled against vinculin and then silver enhanced. (**a**) BSE image view of the uppersurface of Balb c/3T3 fibroblasts displayed gold labels (G) in the permeabilised cells and on the fine filopodia extending between them. (**b**) SE image view of the undersurface of a Balb c/3T3 fibroblast showed only a diffuse image of the cell undersurface (arrows at edge of cell). (**c**) BSE image view of the same Balb c/3T3 fibroblast (C) in resin (R) as in image b showed direct labelling of the vinculin on the undersurface of the cell at the focal adhesions (F).

as dilutions and duration of each step and which blocking agents to use, an acceptable labelling was produced. The upper surface of the permeabilised fibroblasts displayed gold labels in the cells and on the fine filopodia extending between them, with little background labelling on the substrate (Fig. 4a). The undersurfaces of immunogold labelled cells were viewed directly with high emission current BSE imaging through the resin. At low magnifications the cell shapes, with highly stained nuclei, could be seen, though only diffuse ghost images were observed in secondary electron (SE) detection mode under the same conditions. At higher magnifications the general shape of a cell could just be made out with SE imaging using high emission currents (Fig. 4b). Using BSE imaging, with high emission currents, the whole cell shape could be seen with the silver enhanced gold labels on the undersurface of the cell, within the embedding resin, directly on the focal adhesions (Fig. 4c). This showed that vinculin in the adhesion sites remained intact, within the cells, after the substrate had been removed for visualisation of the cell undersurfaces in the embedding resin.

Original images were saved directly in digital form so that no information was lost digitising photographs between imaging the samples and analysing them. When performing image analysis and measurement, the procedure error was found to be up to a maximum of 2%. Some result groups for one material within a test were of normal distribution and some were not, so that the results were logged to produce normal distribution and then analysed with the parametric test. When analysing the cell spread area (Fig. 5), significant differences ($P <= 0.05$) were found between Th and Ti8 and also between S1 and Ti8 with the Balb c/3T3 cells. Significant differences ($P <= 0.05$) were found between Th and S6 and between Th and S8 with L929 cells. There were no significant differences between any of the other samples. Balb c/3T3 cells were seen to have spread more than the L929 cells. When analysing the percentage adhesion of the cells (Fig. 6), significant differences ($P <= 0.05$) were found between Th and all the metals with the Balb c/3T3 cells, but only between Ti1 and Ti8 with L929 cells. L929 cells were observed to have a higher percentage of their total cell surface area covered with adhesion sites compared to the Balb c/3T3 cells.

Adhesion distribution

The binary images produced after the image analysis process, in an overlay upon the original low kV images, showed the orientation of distribution of the focal

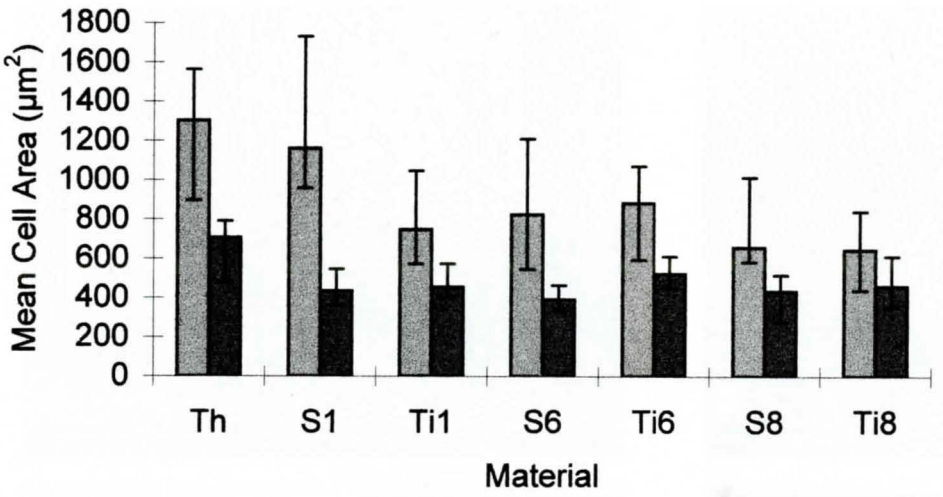

Figure 5. Mean cell area on the different material surfaces for Balb c/3T3 fibroblasts (lighter columns) and L929 fibroblasts (darker columns). The cell spread area was determined for 20 cells for each surface for each type of culture. Bars represent quartiles 1 and 3.

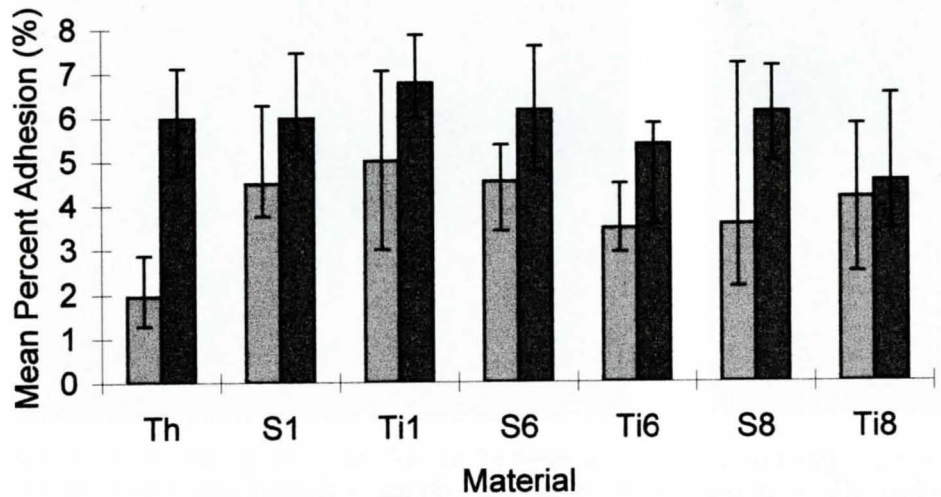

Figure 6. Mean percentage contact of cells by their focal adhesions to the substrate for Balb c/3T3 fibroblasts (lighter columns) and L929 fibroblasts (darker columns). The percentage contact was determined, [cell area (μm^2) / Adhesion area (μm^2) x 100%], for 20 cells for each surface for each type of culture. Bars represent quartiles 1 and 3.

adhesion areas within the cells (Fig. 7c). Focal adhesions were observed to have oriented along the metal ridges or raised microscratches on the test surfaces. This occurred even if the cell itself had not oriented along the line of the ridges (Fig. 7). On fine ridges the adhesion sites were in single lines and were in double or more lines on ridges that were a larger. This was most apparent on the replicas of smoother abraded surfaces. Small outgrowths from the main cell body sometimes did not show focal adhesion orientation, but random distribution on deformity edges (not shown). Not all focal adhesions aligned in rows along ridges. Within some cells, on the same disc as there were cells displaying rows of aligned focal adhesions, the focal adhesions appeared in distinct patches (not shown). There was no orientation of focal adhesion distribution on the Thermanox control, which had no micro-scratches upon the surface (Fig. 2).

Discussion

Immunocytochemistry

Focal contacts are highly organised complexes that maintain the attachment of cells to their substrates, and in combination with the cytoskeleton, are responsible for the general morphological shape of the cells. Immunolocalisation of vinculin, an integral protein on the cytoplasmic side of the focal adhesion (Geiger, 1979), was performed to display the distribution of focal adhesions in the fibroblasts. LM displayed that cells either had focal adhesions over the entire surface or organised around the cell periphery and under the cell centre. This was in agreement with earlier studies. In 1924 it was reported that cell adhesions are restricted to the cell periphery (Goodrich, 1924). Later using SEM, it was observed that the pattern of attachment sites can be uniform in distribution over the whole cell undersurface, but at other times largely peripheral (Revel *et al.*, 1974).

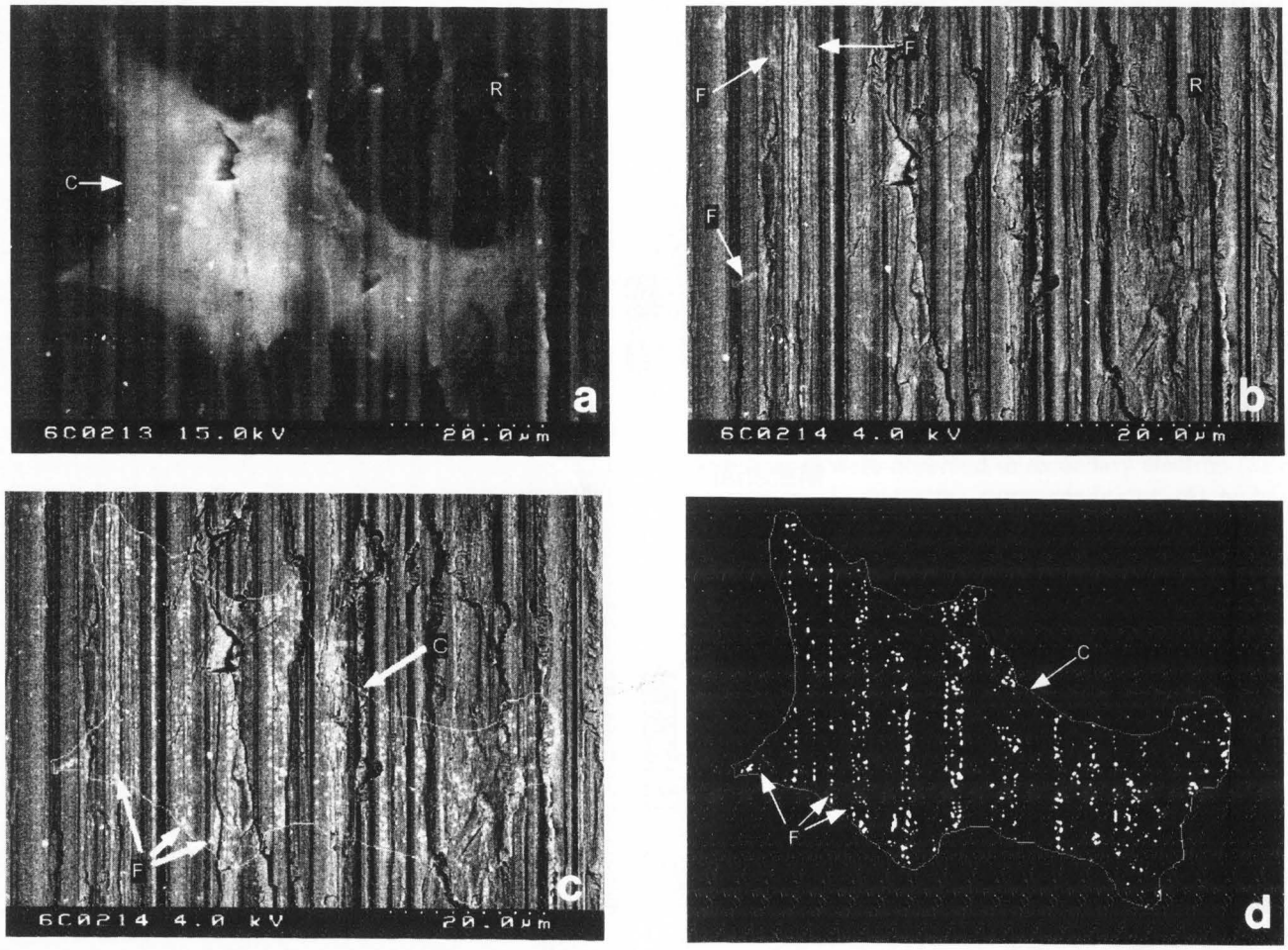

Figure 7. Method of image analysis for quantification of the amount of cell adhesion, using BSE images of the undersurface of a Balb c/3T3 fibroblast (C) cultured on stainless steel (600 grit) and embedded within resin (R). (**a**) 15 kV image of the cell shape and size. A rough resin replica, giving a mirror image of the metal was also evident which displayed ridges and grooves. (**b**) 4 kV image of focal adhesions (F).The fine detail topographical resin replica mirror of the metal was also evident. (**c**) A binary overlay of the cell (C) shape and size and the thresholded points of adhesion (F) displayed the organised pattern of oriented adhesion sites on the resin replica mirror image of the metal ridges. (**d**) After the original grey image was removed, only the binary image of cell shape, size and positions of adhesion sites (F) remained which clearly showed the definitive orientation of the adhesion sites.

Confocal microscopy of the cell-substrate interface had shown that these adhesions were on the undersurface of the cell, with central ones being under the nucleus. The pattern of focal adhesions around the undersurface periphery and under a central nucleus in the present study was in agreement with images of the fibroblasts used for the quantitative adhesion area measurements. Immunoelectron microscopy of the distribution of vinculin has shown that it is confined to the membrane associated contacts (Geiger *et al.*, 1981). Visualisation with the FESEM, using high emission current BSE detection, of silver enhanced immunogold labels attached indirectly to vinculin in the present study showed its distribution through the cells from their upper-surfaces. Direct visualisation of the labels at the cell undersurfaces was also performed by high emission current BSE detection through the embedding resin. Together, the immunolabelling visualised with the LM, confocal microscopy, FESEM and images of remainders of cells from microjet impingement (Richards *et al.*, 1995a) showed that the highly stained small areas visualised on the undersurface of the cells with the FESEM were areas of focal adhesion sites. This showed that the preparation method, used prior to the quantitative measurement of the area of cell adhesion, removed focal adhesion sites, with the embedded cells from the

substrate. Measurement of the highly stained focal adhesion areas could therefore be used as the data for a quantitative comparative method.

The patterns of adhesion were not the same for different cells in a population due to the cells being in different stages of the cell-cycle, as suggested by their different shapes and sizes (i.e., amount of spreading), during the fixation. Cell cycle dependent variation in both cell morphology and their adhesion to substrates is well-documented (Porter *et al*, 1973; Elvin and Evans, 1983; Cross and ap Gwynn, 1987). The time of focal adhesion formation and the time of maintenance of that adhesion are both important factors to be considered when making quantitative cell adhesion comparisons, since focal adhesions are not permanent structures. Abercrombie and Heaysman (1953) showed that the cell-cell contacts, in an active culture, are constantly breaking and reforming and said that similar transitory adhesions occur between a cell and its substrate. With temporary adhesions the exact strength of the adhesion bond is not important, as long as it is greater than that necessary to resist stresses imposed upon it within its local environment.

Adhesion measurement

Mechanical forces were not used to measure the strength of adhesion since when such methods have been used it has been difficult to determine the exact position of molecular failure. Since it was shown that vinculin remained attached to the cells within the embedded resin, focal adhesion sites were still within the cells. Therefore, measurement of the amount of adhesion area, under standard conditions, as a quantifiable method of comparison was valid. The heavy metals stained the structural elements within the cells, which were surrounded by a low density and therefore less stained cellular matrix, which in turn itself was surrounded by low density unstained resin. This differential staining of the cellular material allowed high contrast images of cells embedded within the resin to be produced and of the highly stained adhesion areas surrounded by less stained membrane and matrix to be visualised. Focal adhesions stained to a higher degree than areas of cell membrane-substrate contact, where there was passive contact, due to the high concentration of integral proteins within their structures and the relatively lower concentrations of stainable proteins elsewhere within the cell-substrate interface.

Comparison between the surfaces was made by using the same culturing conditions, the same fixation regime, and the exact same microscope operating conditions. A standard high accelerating voltage of 15 kV was used to show the general cell shape and size and a standard low accelerating voltage of 4 kV was used to display the areas of adhesion. The standard high kV beam penetrated approximately the same depth into resin embedded cells under standardised conditions in different samples. The penetration at a standard low kV would be much less, but also would penetrate to approximately the same depth into resin in different samples. Therefore the amount of cell adhesion from samples on different surfaces was comparable.

The results on mean cell area measurements suggest that there was a tendency towards cells spreading more on the smoother surfaces than on the rougher ones. This had previously been indicated when it was observed that cells have a flatter morphology on smooth titanium surfaces than on rougher surfaces (Könönen *et al.*, 1992). The mean percentage adhesion measurements show however that there was no difference in the amount of adhesion between the different roughnesses used in this study. The static *in vitro* results imply that under conditions of no shear, surface roughness has a negligible effect on the total amount of the cell adhesion to the surface. The ratio of mean focal adhesion area per cell to the mean cell spread area was the same for both metals tested with both cell types, though different between the two cell type groups. This suggests a relationship, within a particular cell type, between the number of focal adhesion sites and the spread size of the cell. The next step in the application of this technique will be look at fixed, stained and embedded samples from an *in vivo* situation where shear, muscle movements and a whole range of other forces act upon the cells.

With respect to the design of implant biomaterials, which are in contact with soft tissues, by taking note of the above observations and the results of other investigations, the nature of an optimal implant surface can be speculated upon. Very smooth surfaces, such as electropolished stainless steel, *in vivo* cause fibroblasts to respond by producing a collagen capsule between the soft tissues and the implant (Brunette, 1988). Electropolished stainless steel plates, *in vivo,* induce thicker adjacent tissue layers than do anodised titanium plates *in vivo* (Ungersböck *et al.*, 1996). *Staphylococcus aureus* is the most common pathogen found in infections of the interfaces between metal biomaterial and bone or soft tissue (Gristina, 1987). The diameter of *Staphylococcus aureus* is about 0.8 μm. Rough surfaces are especially prone to infection (Brunette, 1988). The results of these studies, taken along with those of the current study, suggest that there should exist an optimal roughness, between the roughness that is prone to infection and a smoothness that induces thicker capsule formation. If capsule formation is minimal on the 'optimal roughness surface', vascularisation to that surface could be obtained which would minimise the

chances of infection. It is hoped that *in vivo* studies will bear this hypothesis out.

Adhesion distribution

The initial alignment of actual cells to an ultramicroscopic interface was first observed in 1941 and termed contact guidance (Paul Weiss, 1941). In this present study it was observed that the fibroblast cells aligned their adhesion sites to the ridges. This consequently causes cytoskeletal structures to form along them. This is in agreement with numerous publications on fibroblast cell orientation and alignment. Fibroblasts acquire orientation of their bodies parallel to grooves on surfaces (Rovensky *et al.*, 1971). Fibroblasts and epithelial cells bridge over small grooves (2-10 μm wide), confining their focal adhesions to intervening ridges, which causes their alignment and the alignment of the whole cell (Ohara and Buck, 1979). Clark *et al.* (1990) had also observed that cells on deeper grooved substrata bridge over the grooves but are not aligned in any way, so that confinement of adhesion to the ridges does not have to result in cell alignment. They also stated that many of Ohara and Buck's original micrographs show bridging without cell alignment. They suggested that the factor determining protrusion success of cells is their cytoskeletal flexibility. Protrusions made against the grain of the substrate are less able to form stable lamellipodia that can exert traction. Therefore the cells' expansion across the grooves is inhibited and the probability of success of expansion in the direction of the grooves depends on ridge spacing and groove depth.

Our results agree with those of Clark *et al.* (1990), with adhesion sites distributed in alignment to the ridges when cell bodies were not. We suggest that fibroblast focal adhesions have to attach and therefore align to the ridges or discontinuities, whether the cell bodies do or not. This obviously depends on the definition of a ridge and the periodicity of ridges and grooves. This present work does not attempt to answer that, as the study of cell orientation was not within the original aims of the project. The effects of defined grooved surfaces on fibroblast cell orientation have been reported on numerous occasions (Brunette 1986, 1988; Dunn and Brown, 1986; Inoue *et al.*, 1987; Cheroudi *et al.*, 1991; Oakley and Brunette, 1993; Abiko and Brunette, 1993; Meyle *et al.*, 1994; Green *et al.*, 1994; Den Braber *et al.*, 1995, 1996a,b; Wojciak-Stothard *et al.*, 1995). However, this was not the main subject area of this paper but the results obtained are in agreement with the published work. The technique presented here could be applied to quantifying the formation of and studying the distribution of focal adhesions from any cell type that forms them on a variety of substrate materials.

Conclusion

An *in vitro*, reliable and reproducible, testing procedure for measuring quantitatively the percentage of cell surface area adhering to biomaterials is presented. The results of the technique show that surface roughness has a negligible effect on the total area of fibroblast adhesion *in vitro*, under static conditions of no shear, with the surfaces and the cell lines tested. The method is also suggested to be of use for studies of focal adhesion orientation within cells to substrates of varying topography and topology.

Acknowledgements

The authors would like to thank Professor Stephan Perren for his encouraging support and questions during the numerous presentations of the development of this work; Professor Schneider, the new director of AO/ASIF, for the critical review of the manuscript; Dr. Keita Ito for help with statistical analysis techniques. The original development of the methods described in this paper was funded by AO/ASIF Research Commission grant #93-G14. This study was in part supported by the Swiss National Science Foundation grant # 32-4931596.

References

Abercrombie M, Heaysman JEM (1953) Observations of the social behaviour of cells in tissue culture. I. Speed of movement of chick heart fibroblasts in relation to their mutual contacts. Exp Cell Res **5**: 111-131.

Abiko Y, Brunette DM (1993) Immunohistochemical investigation of tracks left by the migration of fibroblasts on titanium surfaces. Cell Mater **3**: 161-170.

Ambrose EJ (1956) A surface contact microscope for the study of cell movements. Nature **178**: 1194.

Bell GI (1978) Models for the specific adhesion of cell to cells. Science **200**: 618-627.

Bongrand P, Goldstein P (1983) Reproducible dissociation of cellular aggregates with a wide range of calibrated shear forces: application to cytolytic lymphocyte-target cell conjugates. J Immunol Meth **58**: 209-224.

Brunette DM (1986) Fibroblasts on micro-machined substrata orient hierarchically to grooves of different dimensions. Exp Cell Res **164**: 11-26.

Brunette DM (1988) The effects of implant surface topography on the behaviour of cells. Int J Oral Maxillofac Impl **3**: 231-246.

Bundy KJ, Rahn BA, Schlegel U, Geret V, Perren S (1991) Factors affecting soft tissue adhesion to

biomaterials. In: Transactions 17th Ann Meeting Soc Biomaterials. Parsons JR (ed). Society for Biomaterials, Algonquin, IL. p 229.

Bundy KJ, Roberts OC, O'Connor KO, Mcleod V, Rahn BA (1994) Quantification of fibroblast adhesion to biomaterials using a fluid mechanics approach. J Mat Sci Mat Med **5**: 500-502.

Cheroudi B, Gould TR, Brunette DM (1991) A light and electron microscopic study of the effects of surface topography on the behaviour of cells attached to titanium coated percutaneous implants. J Biomed Mat Res **25**: 387-405.

Clark P, Connolly P, Curtis ASG, Dow JAT, Wilkinson CDW (1990) Topographical control of cell behaviour. II. Multiple grooved substrata. Development **108**: 635-644.

Coman DR (1944) Decreased mutual adhesiveness, a property of cells from squamous cell carcinomas. Cancer Res **4**: 625-629.

Cornell R (1969) Cell-substrate adhesion during cell culture. Exp Cell Res **58**: 289-295.

Cross SJ, ap Gwynn I (1987) Adhesion and the cell cycle in cultured L929 and CHO cells. Cytobios **50**: 41-62.

Curtis ASG (1964) The mechanism of adhesion of cells to glass. J Cell Biol **20**: 199-215.

Davies PF, Robotewskyj A, Griem ML (1993) Endothelial cell adhesion in real time: measurements *in vitro* by tandem scanning confocal image analysis. J Clin Invest **91**: 2640-2652.

Den Braber ET, Ruijter JE, Smits HTJ, Ginsel LA, von Recum AF, Jansen JA (1995) Effect of parallel surface microgrooves and surface energy on cell growth. J Biomed Mat Res **29**: 511-518.

Den Braber ET, Ruijter JE, Smits HTJ, Ginsel LA, von Recum AF, Jansen JA (1996a) Quantitative analysis of cell proliferation and orientation on substrata with uniform parallel surface micro-grooves. Biomaterials **17**: 1093-1099.

Den Braber ET, Ruijter JE, Smits HTJ, Ginsel LA, von Recum AF, Jansen JA (1996b) Quantitative analysis of fibroblast morphology on microgrooved surfaces with various groove and ridge dimensions. Biomaterials **17**: 2037-2044.

Dunn GA, Brown AF (1986) Alignment of fibroblasts on grooved surfaces described by a simple geometric transformation. J Cell Sci **83**: 313-340.

Elvin P, Evans CW (1982) The adhesiveness of normal and SV40 transformed Balb/c 3T3 cells: Effects of culture density and shear rate. Eur J Cancer Clin Oncol **18**: 669-675.

Elvin P, Evans CW (1983) Cell adhesiveness and the cell cycle. Correlation in synchronised Balb/C 3T3 cells. Biol Cell **48**: 1-10.

Geiger B (1979) A 130K protein from chicken gizzard: its localisation at the termini of microfilament bundles in cultured chicken cells. Cell **18**: 193-205.

Geiger B, Dutton AH, Tokuyasu KT, Singer SJ (1981) Immunoelectron microscope studies of membrane microfilament interactions: Distribution of α-actinin, tropomyosin and vinculin in intestinal brush border and chicken gizzard smooth muscle cells. J Cell Biol **91**: 614-628.

Goodrich HB (1924) Cell behaviour in tissue cultures. Biol Bull **46**: 252-262.

Green AM, Jansen JA, Van der Waerden JPCM, Von Recum AF (1994) Fibroblast response to microtextured silicone surfaces: Texture orientation into or out of the surface. J Biomed Mat Res **28**: 647-653.

Gristina AG (1987) Biomaterial-centred infection: Microbial adhesion versus tissue integration. Science **237**: 1588-1595.

Hertl W, Ramsey WS, Nowlan ED (1984) Assessment of cell substrate adhesion by a centrifugal method. In Vitro **20**: 796-801.

Hodges GM, Smolira MA, Livingston DG (1984) Scanning electron microscope immunocytochemistry in practice. In Immunolabelling for electron microscopy. Polak JM, Varndell IM (eds). Elsevier Science Publishers, Amsterdam, pp 189-233.

Holgate CS, Jackson P, Cowen PN, Bird CC (1983) Immunogold silver staining: a new method of immunostaining with enhanced sensitivity. J Histochem Cytochem **31**: 938-944.

Hunter A, Archer CW, Walker PS, Blunn GW (1995) Attachment and proliferation of osteoblasts and fibroblasts on biomaterials for orthopaedic use. Biomaterials **16**: 287-295.

Inoue T, Cox JE, Pilliar RM, Melcher AH (1987) Effect of the surface geometry of smooth and porous coated titanium alloy on the orientation of fibroblasts *in vitro*. J Biomed Mat Res **21**: 107-126.

Isenberg G, Rathke PC, Hülsmann N, Franke WW, Wohlfahrth-Botterman KE (1976) Cytoplasmic actomyosin fibrils in tissue culture cells - Direct proof of contractibility by visualisation of ATP-induced contraction in fibrils isolated by laser microbeam dissection. Cell Tissue Res **166**: 427-443.

Könönen M, Hormia M, Kivilahti J, Hautaniemi J, Thesleff I (1992) Effect of surface processing on the attachment, orientation, and proliferation of human gingival fibroblasts on titanium. J Biomed Mat Res **26**: 1325-1341.

Lotz MM, Burdsal CA, Erickson HP, McClay DR (1989) Cell adhesion to fibronectin and tenascin: Quantitative measurements of initial binding and subsequent strengthening response. J Cell Biol **109**: 1795-1805.

Meyle J, Gultig K, Brich M, Hammerle H, Nisch W (1994) Contact guidance of fibroblasts on bio-material surfaces. J Mat Sci Mat Med **5**: 463-446.

Oakley C, Brunette DM (1993) The sequence of alignment of microtubules, focal contacts and actin filaments in fibroblasts spreading on smooth and grooved titanium substrata. J Cell Sci **106**: 343-354.

Ohara PT, Buck RC (1979) Contact guidance *in vitro*: A light, transmission, and scanning microscopic study. Exp Cell Res **121**: 235-249.

Porter K, Prescott D, Frye J (1973) Changes in surface morphology of CHO cells during the cell cycle. J Cell Biol **57**: 815-836.

Revel JP, Hoch P, Ho D (1974) Adhesion of culture cells to their substratum. Exp Cell Res **84**: 207-218.

Richards RG, ap Gwynn I (1995) Backscattered electron imaging of the undersurface of resin-embedded cells by field emission scanning electron microscopy. J Microsc **177**: 43-52.

Richards RG, ap Gwynn I, Bundy KJ, Rahn BA (1995a) Microjet impingement followed by scanning electron microscopy as a qualitative technique to compare cellular adhesion to various biomaterials. Cell Biol Int **19**: 1015-1024.

Richards RG, Rahn BA, ap Gwynn I (1995b) Scanning electron microscopy of the undersurface of cell monolayers grown on metallic implants. J Mat Sci Mat Med **6**: 120-124.

Rosenberg MD (1960) Microexudates from cells grown in tissue culture. Biophys J **1**: 137-159.

Rovensky YA, Slavnaja IL, Vasiliev JM (1971) Behaviour of fibroblast-like cells on grooved surfaces. Exp. Cell Res **65**: 193-201.

Truskey GA, Pirone JS (1990) The effect of fluid shear stress upon cell adhesion to fibronectin treated surfaces. J Biomed Mat Res **24**: 1333-1353.

Truskey GA, Proulx TL (1993) Relationship between 3T3 cell spreading and the strength of adhesion on glass and silane surfaces. Biomaterials **14**: 243-254.

Ungersböck A, Pohler OEM, Perren SM (1996) Evaluation of soft tissue reactions at the interface of titanium limited contact dynamic compression plate implants with different surface treatments: an experimental sheep study. Biomaterials **17**: 797-806.

Vaishnav RN, Patel DJ, Atabek MD, Deshpande F, Plowman F, Vossoughi J (1983) Determination of the local erosion stress of the canine endothelium using a jet impingement method. J Biomech Eng **105**: 77-83.

Van Kooten TG, Schakenraad JM, Van der Mei HC, Busscher HJ (1991) Detachment of human fibroblasts from FEP-Teflon surfaces. Cells Mater **1**: 307-316.

Van Kooten TG, Schakenraad JM, Van der Mei HC, Busscher HJ (1992) Development and use of a parallel-plate flow chamber for studying cellular adhesion to solid surfaces. J Biomed Mat Res **26**: 725-738.

Van Kooten TG, Schakenraad JM, Van der Mei HC, Dekker A, Kirkpatrick CJ, Busscher HJ (1994) Fluid shear induced endothelial cell detachment from glass - influence of adhesion time and shear stress. Med Eng Phys **16**: 506-512.

Weiss L (1961) The measurement of cell ad-hesion. Exp Cell Res **8**: 141-153.

Weiss L, Coombs RA (1963) The demonstration of rupture of cell surfaces by an immunological technique. Exp Cell Res **30**: 331-338.

Weiss P (1941) Nerve patterns: The mechanics of nerve growth. Growth **5**: 163-203.

Wojciak-Stothard B, Curtis ASG, Monaghan W, McGrath M, Sommer I, Wilkinson CDW (1995) Role of the cytoskeleton in the reaction of fibroblasts to multiple grooved substrata. Cell Motil Cytoskel **31**: 147-158.

Discussion with Reviewers

G.M. Roomans: I sorely miss a TEM micrograph showing the situation in Fig.1, and, at higher magnification, the attachment sites.
Authors: In a way we agree with you here, but the time and effort required to attain a suitable image that is similar to Fig. 1, passing through numerous focal adhesion sites that were attached to the surface is out of proportion to the contribution it would make. It would not tell us much more about the situation.

J.M. Schakenraad: Why do you not use antibiotics in cell culturing?
Authors: We have not had an infection without antibiotics, and therefore antibiotics are not used. Use of antibiotics slows the proliferation of the fibroblasts and produces uncharacteristic shapes. Therefore, more natural conditions for the cells are achieved by not using them.

J.M. Schakenraad: You certainly know that surface roughness is often used to create better mechanical "resistance" between biomaterial and tissue. Although I do not understand that this does not mean that this will result in better cellular adhesion (or more focal adhesion sites) it does implicate that macro-roughness can not be abandoned. What is your opinion?
Authors: Though the *in vitro* results did not show a difference between the roughnesses tested, we think that *in vivo* results would. These *in vitro* results were obtained under static conditions, with no shear. Shear generating coditions are known to occur *in vivo*. We think that rougher surfaces will cause more fibroblast

adhesion in both the *in vivo* situation and in the *in vitro* situation, when there are shear forces present. Macro-roughness (defined as being greater than single cell dimensions) was not investigated in this study but we feel it possibly could have an affect on connective tissue adhesion to the implant as a whole, where it may protect tissue from the effects of shear forces.

J.A. Jansen: This paper describes a new technique to measure cell adhesion to biomaterials using FESEM. The advantage of this technique above conventional confocal laser scanning microscopy (CLSM) is unclear. Also using CLSM, the occurrence of vinculin can be studied with less chance on artefacts due to drying and separation techniques.
Authors: Firstly we do not have a CLSM. We believe we have shown that the method described shows certain resolution advantages over any light microscopy technique at the interface of the cell to substrate. There is no necessity for immunocytochemical labelling of adhesion sites, with the possibility of errors due to incomplete labelling. All focal contacts, as they all stain with the heavy metal, will show up and can be counted. When we have performed immunocytochemical labelling of adhesion sites, the labelled vinculin within the focal adhesion has always remained within the resin block after substrate removal. This indicates that there are probably no artefacts due to separation of the substrate. The focal adhesion sites are stained before any dehydration process and none will disappear during dehydration.

J.A. Jansen: In Fig. 3a the authors show that vinculin is mainly present at the cell periphery. In Fig. 7d the authors show that the vinculin occurs mainly on the surface ridges with an almost uniform distribution over the whole cell. These results seem to contradict each other. How can this be explained?
Authors: These results do not contradict each other, since in one situation the cell is on a smooth plastic surface, while in the other case the cell is on a rough metal surface with oriented ridges. For a general comment, adhesion site positions on smooth surfaces may be either uniformly distributed under the whole of the cell or observed under the nucleus and around the cell periphery (Revel *et al.*, 1974). The precise situation in any individual cell is also probably related to the cell cycle stage of the cell.

J.A. Jansen: The authors suggest that the occurrence of vinculin is a measure for cell adhesion and therefore a measure of biocompatibility of an implant material. This theory can be doubted. Vinculin is just one component of the whole cascade of proteins which form the connection between the substrate surface and the cytoskeleton (nucleus). This cascade of proteins also plays an important role in the signalling in and out of a cell. Perhaps this last function of an adhesion structure is even more important than adhesion itself.
Authors: We are well aware of the role of vinculin in the cytoskeleton. We have not suggested that the occurrence of vinculin is a specific measure of cell adhesion. All we have done is to show that vinculin is present within the heavy metal stained focal adhesion sites. This simply verifies their identification, since it is confined to the membrane associated contacts (Geiger *et al.*, 1981). Measurement and counting of sites was performed on the heavy metal stained sites only. The fact that backscattered electron signal emerges, under the set conditions applied, from only a short depth (approximately a few hundred nanometres) from within the specimen restricts the cellular structures from which they could emerge to the adhesive structures of the cell.

G.M. Roomans: The method requires that the entire attachment site is in the block that is examined in the microscope, and that nothing remains on the biomaterial. Are you sure that this is the case? How can you check this?
Authors: The method does not require the entire adhesion complex to be present within the removed resin block. The bulk of the heavy metal staining is probably within the integral proteins of the adhesion site and the attached actin filaments. We have also checked, with both low voltage SE and BSE imaging, the removed substrate for attached cellular debris, but found none.

G.M. Roomans: I wonder whether only the lateral size of the attachment site is relevant, or whether the depth of the site may be important too.
Authors: Using the set microscope operating conditions we always penetrate the sample to approximately the same depth with the electron beam. Therefore for comparison this problem is eliminated. Also, the structure of the focal adhesion is well known and the intensity of staining should reflect the number of individual contact elements made.

G.M. Roomans: Fig. 4b indicates that the surface of the block is not smooth. From the description in Materials and Methods I gather that only the metal was polished, not the plastic block. Do irregularities of the surface compromise the BSE image at low kV?
Authors: Firstly the block in 4b was not a normal block since the cells had been labelled, viewed from above, then embedded and viewed from below. This caused poor separation forming irregularities. The depth from which BSE images are obtained should follow the

surface contours.

G.M. Roomans: The choice of accelerating voltages 4 kV (to see the attachment sites) and 15 kV (to see the whole cell) must be based on: (1) an assumption about the penetrating power of the beam, (2) an assumption on the size of the cell and the attachment sites. Neither is presented or discussed explicitly.

Authors: The assumption on which the choice of these two beam energies is taken from our earlier published work on the behaviour of BSE images at different beam energies (Richards and ap Gwynn, 1995c). Trials revealed that 15 kV penetrates sufficiently into the resin to reveal the whole outline of the cell and 4 kV will only show the stained adhesion sites.